Organic & Biomolecular Chemistry

PAPER

View Article Online
View Journal

Published on 23 February 2016. Downloaded by Johns Hopkins University on 03/03/2016 18:08:06.

Cite this: DOI: 10.1039/c5ob02309b

Innocent BN bond substitution in anthracene derivatives†

H. L. van de Wouw, J. Y. Lee, M. A. Siegler and R. S. Klausen*

Received 9th November 2015,
Accepted 23rd February 2016

DOI: 10.1039/c5ob02309b

www.rsc.org/obc

Extended azaborine heterocycles are promising biomedical and electronic materials. Herein we report the synthesis of a novel family of azaborine anthracene derivatives and their structural, electrochemical and spectroscopic characterization. We observe that the properties of these materials are remarkably similar to the parent hydrocarbons, suggesting the innocence of the CC to BN bond substitution. Our results support the prospective stability to long-term usage of extended azaborines and the feasibility of using such materials in device applications.

Introduction

We report the synthesis and characterization of new extended azaborine derivatives and the remarkable structural, optical and electronic similarity of these heterocycles to anthracene.

The unusual stability of some cyclic conjugated organic structures, or aromaticity, is a foundational concept in organic chemistry.[1] Main group organometallic compounds containing Hückel's rule number of π electrons were first synthesized by Dewar in 1958.[2] In recent years,[3] new synthetic approaches courtesy of Liu,[4] Ashe,[5] and Molander[6,7] have energized research in the area of BN-heterocycles and both fundamental and applied research have expanded in scope. Liu and Chrostowska have extensively investigated the electronic structure of these systems.[8,9] Potential applications in materials science, including hydrogen storage,[10] organic light-emitting diodes (OLEDs),[11] and organic field effect transistors[12] (OFETs) have been explored. The biomedical relevance of azaborine heterocycles is actively investigated.[13,14] BN materials have been extensively reviewed.[15–18]

The continued development of these materials depends on predictive structure–function relationships as theoretical accounts have suggested that not all CC to BN bond substitutions are equal.[19] In an effort to systematically characterize structure-dependent properties, we target a series of extended azaborine derivatives (BN anthracenes) with aryl rings exocyclic to the BN heterocycle (Fig. 1). We show that the B-aryl anthracenes in which the 1,2-positions are substituted with the BN bond have optical and electronic properties consistent with delocalization. The observed trends closely parallel anthracene itself and point to the remarkable innocence of some CC to BN bond substitutions.

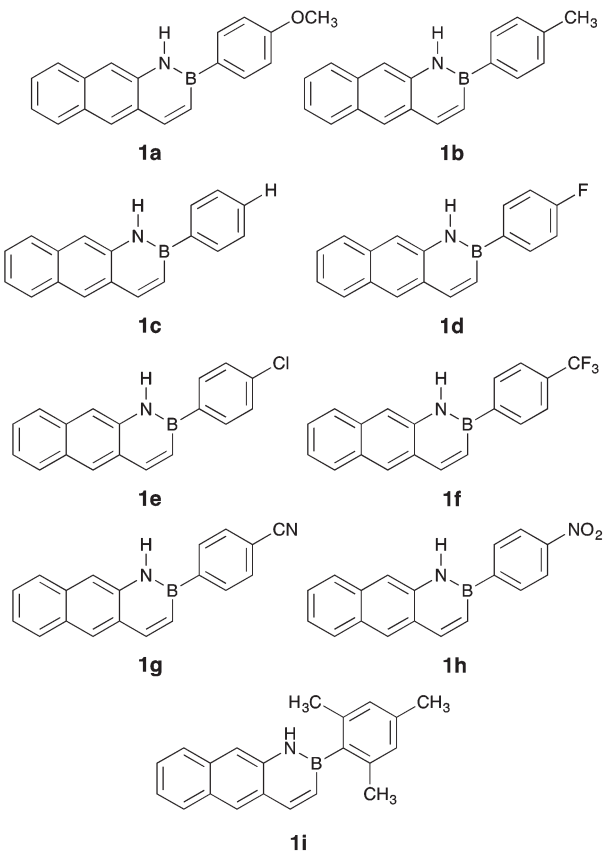

Fig. 1 Chemical structures of known (1c) and new (1a–b, 1d–i) BN anthracenes synthesized in this work.

Department of Chemistry, Johns Hopkins University, Baltimore, MD 21218, USA. E-mail: klausen@jhu.edu

† Electronic supplementary information (ESI) available: Experimental details and spectroscopy. CCDC 1435441–1435446, 1453177 and 1453178. For ESI and crystallographic data in CIF or other electronic format see DOI: 10.1039/c5ob02309b

Published on 23 February 2016. Downloaded by Johns Hopkins University on 03/03/2016 18:08:06.

Results and discussion

B-aryl anthracene synthesis

Dewar's pioneering synthesis of BN naphthalene *via* borylation of 1,2-aminostyrene with trichloroborane (Fig. 2) inspires recent work on extended azaborine derivatives.[20] Molander reported the one-pot synthesis of functionalized BN naphthalene derivatives by the *in situ* generation of organodichloroboranes from bench-stable potassium organotrifluoroborate salts.[6,7] Liu recently reported the first synthesis of BN anthracene by adaptation of Dewar's borylation and reduction sequence (Fig. 3a).[21] The Liu synthesis begins with conversion of 2-amino-3-naphthoic acid **2** to iodoarene **3** by a Sandmeyer reaction–Curtius rearrangement sequence. The key intermediate **4** is obtained after a Suzuki vinylation with potassium vinyltrifluoroborate that proceeds in 65% yield.

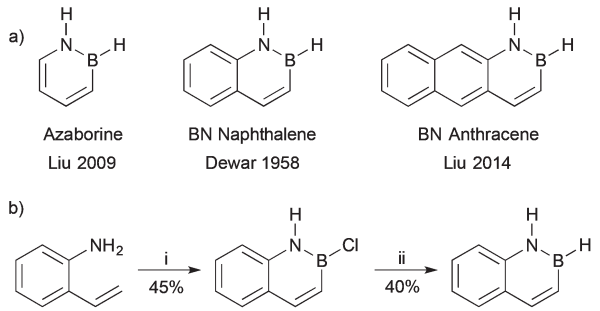

Fig. 2 (a) Linearly fused extended azaborine derivatives. (b) Dewar's synthesis of BN naphthalene. (i) BCl_3, PhH, 80 °C, 45%; (ii) LAH, Et_2O, 40%. LAH = lithium aluminium hydride.

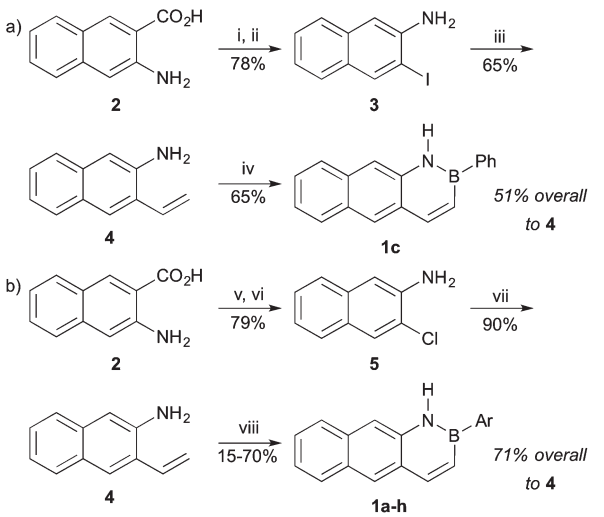

Fig. 3 (a) Liu synthesis of BN anthracene **1c**. (i) $NaNO_2$, KI, HCl, 88%. (ii) DPPA, NEt_3, H_2O, 89%. (iii) Pd(dppf)Cl_2, NEt_3, potassium vinyl trifluoroborate, 65%. (iv) $PhBCl_2$, toluene, 110 °C, 65%. (b) Klausen synthesis of BN anthracene library. (v) $NaNO_2$, H_2SO_4; CuCl, HCl, 86%. (vi) DPPA, NEt_3, H_2O, 92%. (vii) Vinylboronic acid MIDA ester, SPhos, $Pd(OAc)_2$, K_3PO_4, 90%. (viii) $ArBF_3K$, $SiCl_4$, NEt_3, toluene–CPME, 100 °C, 15–70%. DPPA = diphenylphosphoryl azide; MIDA = *N*-methyliminodiacetic acid; SPhos = 2-dicyclohexylphosphino-2′,6′-dimethoxybiphenyl; CPME = cyclopentyl methyl ether.

Towards the synthesis of our target library of compounds, we applied Molander's one-pot reaction conditions to Liu's 2-amino-3-vinylnaphthalene intermediate **4** (Fig. 3b). We also report a higher yielding synthetic route to key intermediate **4**. We subject 2-amino-3-naphthoic acid **2** to the sequence of a Sandmeyer reaction with cuprous chloride[22] and a Curtius rearrangement to yield chloroarene **5**. A Suzuki reaction between chloroarene **5** and vinylboronic acid MIDA ester[23] catalysed by $Pd(OAc)_2$/SPhos proceeds in 90% yield. The overall yield of **4** from commercially available **2** is 71%. While compound **1c** was recently reported by Liu *et al.*, the other BN anthracenes in this study are unknown.

Single crystal X-ray crystallography

Single crystals of B-aryl anthracenes were grown from solution at room temperature as described in the ESI.† Key crystallographic parameters for the structures of **1b**, **1c**, **1d**, **1f**, **1g**, **1h**, and **1i** are summarized in Table 1.

Across the series, the length of the BN bond remains statistically identical at *ca.* 1.42 Å (Table 1). This bond length is comparable to the 1.44 Å bond length of borazine ($B_3N_3H_6$).[24] It is intermediate between the BN single bond length (1.51 Å) and the BN double bond length (1.31 Å).[25] Intermediate bond lengths and partial bond order are experimental hallmarks of cyclic delocalization, or aromaticity: the bond lengths in benzene are *ca.* 1.40 Å, intermediate between the carbon–carbon single bond length of *ca.* 1.54 Å and the carbon–carbon double bond length of *ca.* 1.34 Å.

In all BN anthracenes we have prepared, the crystal packing arrangement is herringbone (Fig. 4a and b), the same arrangement as in anthracene.[26,27] That the BN anthracenes should have a similar crystal packing structure to anthracene is not obvious. Anthracene is a high symmetry hydrocarbon with zero net molecular dipole. Herringbone packing maximizes quadrupolar interactions between the positively charged aromatic edges and the negatively charged aromatic face. In contrast, the polar BN bond desymmetrizes the BN anthracenes and in principle the bond dipole moment could influence

Table 1 Selected torsion angles and bond distances for **1b**, **1c**, **1d**, **1f**, **1g**, **1h**, and **1i**. The values and esd in Table 1 were directly obtained from the experimental cif files

Compound	Aryl Group	∠N1–B1–C13–C14[a] (°)	N1–B1 (Å)
1b[c]	4-$(CH_3)C_6H_4$	−6.6(6), 7.5(5)	1.421(5), 1.418(5)
1c	Ph	−5.0(3)	1.426(3)
1d	4-FC_6H_4	−5.3(2)	1.423(2)
1f	4-$(CF_3)C_6H_4$	5.4(2)	1.4175(18)
1g	4-$(CN)C_6H_4$	5.4(2)	1.419(2)
1h	4-$(NO_2)C_6H_4$	−2.7(2)	1.4207(16)
1i	Mes[b]	−84.7(2)	1.418(2)

[a] Torsion angle. [b] Mes = mesityl = 2,4,6-trimethylphenyl. [c] The two values of the torsion angles and bond distances are given for the two crystallographically independent molecules.

 This journal is © The Royal Society of Chemistry 2016

Published on 23 February 2016. Downloaded by Johns Hopkins University on 03/03/2016 18:08:06.

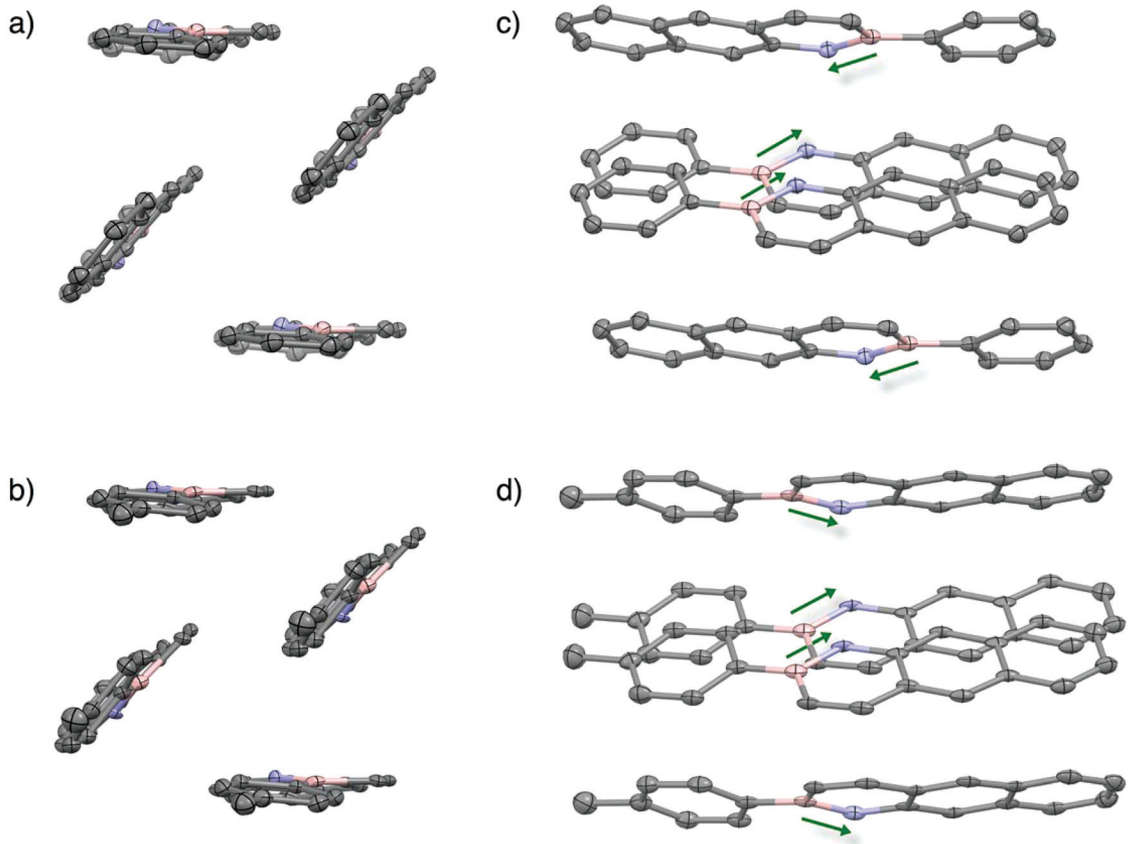

Fig. 4 Representative crystal packing of BN anthracenes. (a) Herringbone packing of *B*-Ph **1c**. (b) Herringbone packing of *B*-Tol **1b**. (c) Approximately antiparallel orientation of **1c** molecules. (d) Approximately parallel orientation of **1b** molecules. The BN dipole is indicated with a green arrow. Displacement ellipsoids are given at 50% probability level. Disorder and hydrogens omitted for clarity. Grey = carbon; blue = nitrogen; pink = boron.

molecular interactions. That it does not again points to the innocence of a single BN bond substitution in the aromatic core. Furthermore, some structures are disordered so that two neighbouring molecules may be either aligned parallel or antiparallel with respect to the BN bond (Fig. 4c and d). That there is no preference between parallel and antiparallel orientations shows the minimal influence of the bond dipole moment on the packing structure.

In both ours and Liu's crystal structures of **1c**, the absolute value of the torsion angle between the exocyclic ring and the extended core is 5°. In fact, all BN anthracene structures but **1i** show that the exocyclic B-aryl group is co-planar with the anthracene framework (Fig. 5). The absolute values of the torsion angles vary from 2.7 to 7.5° (Table 1). In contrast, in the crystal structure of the heterocycle **1i**, the mesityl group is almost orthogonal to the plane of the BN anthracene (∠ = *ca.* 85°). The orthogonal mesityl group is expected, as steric hindrance between the *ortho* methyl groups and the anthracene core prevents a coplanar arrangement.

2-Arylanthracene syntheses and Crystal structures

We hypothesized that the exocyclic B-aryl ring is coplanar with the anthracene core to stabilize the empty p-orbital on boron. As a control, we synthesized 2-phenylanthracene **8a**, which has a full octet. We find that Suzuki coupling of commercially available 2-chloroanthroquinone and an arylboronic acid[28] followed by quinone reduction[29] yields 2-arylanthracenes **8a–c** (Fig. 6).

The crystal structure of **8a** shows a coplanar arrangement (∠C20–C15–C13–C14 = −6.7(4)°) of the anthracene and exocyclic phenyl ring, which does not support the hypothesis that coplanarity is a result of a favourable driving force related to the empty boron orbital. A herringbone crystal packing structure in which individual molecules are antiparallel is observed for compound **8a**. This result again highlights the similarity of BN anthracenes to aromatic hydrocarbons.

Calculated structure

For more insight into the coplanar geometry, we compared the optimized geometry of isolated molecules in vacuum to the molecular crystal structures using density functional theory calculations (CAM B3LYP/6-311G(d,p)). At this level of theory, all B-aryl anthracenes and 2-arylanthracenes were predicted to have a noncoplanar structure with the key torsion angle varying between 25 and 40° (see Table S-5†). Calculations also accurately predict a BN bond length of 1.42 Å. The difference

Published on 23 February 2016. Downloaded by Johns Hopkins University on 03/03/2016 18:08:06.

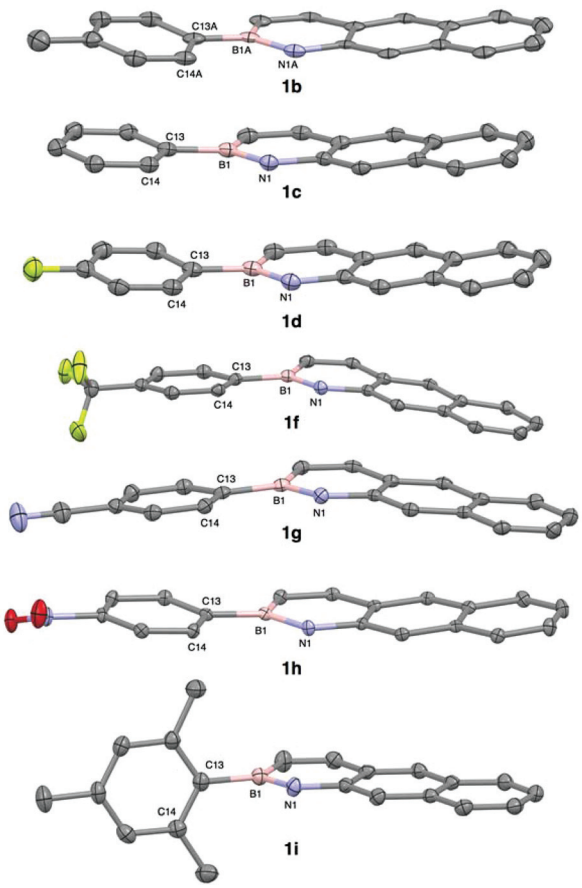

Fig. 5 Displacement ellipsoid plots (50% probability level) of BN anthracenes at 110(2) K. Disorder and hydrogens omitted for clarity. Grey = carbon; blue = nitrogen; pink = boron; green = fluorine, red = oxygen.

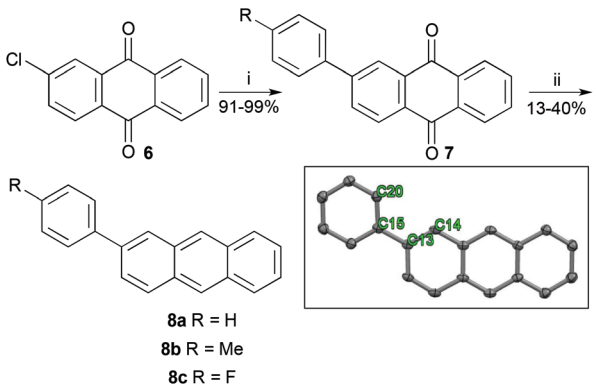

Fig. 6 Synthesis of 2-arylanthracenes **8a–c**. (i) $ArB(OH)_2$, $Pd(PPh_3)_4$, K_2CO_3, toluene, 110 °C, 91–99%; (ii) LAH, HCl, THF (repeat twice), 13–40%. LAH = lithium aluminium hydride. Inset shows molecular structure of **8a** determined by single crystal XRD. Displacement ellipsoid plot (50% probability level) of **8a** at 110(2) K. Grey = carbon. Disorder and hydrogens omitted for clarity. Atoms C14, C13, C15, and C20 are labelled. The torsion angle defined by these carbons is −6.7(4)°.

between the optimized *in vacuo* structure and the experimentally determined crystal structure suggests crystal packing and intermolecular forces drive coplanarity. We identify short edge-face contacts between the exocyclic ring face and aromatic edges of neighbouring molecules in the crystal packing structure.

Absorbance spectroscopy

Solution phase absorbance spectroscopy of BN anthracenes suggests these materials can be divided into two classes.

In the first class are the coplanar derivatives **1a–g**. These materials all have an onset of absorbance around 400 nm, corresponding to an optical bandgap of about 3.10 eV (Table 2, entries 1–7). In the second class are BN anthracene itself and mesityl derivative **1i** (entries 8 and 9). These two materials are slightly blue-shifted relative to the coplanar derivatives with an onset of absorbance at 390 nm ($E_g \approx$ 3.16 eV).

Clearly, the exocyclic ring positively influences the properties of the entire system when it achieves a coplanar arrangement. The degree of red-shifting achieved in the BN anthracenes is remarkably similar to that observed in the hydrocarbon scaffold as well. We find that 2-arylanthracenes **8a–c** are also about 10 nm red-shifted relative to anthracene itself (entries 10–13) and that the optical band gaps of **8a–c** are similar to their BN analogs.

Electrochemistry

BN anthracene electrochemistry closely parallels anthracene's electrochemistry. In dimethylformamide at room temperature, for BN anthracenes **1a–g**, we observe a reversible or quasireversible reduction peak at about −2.5 V *vs.* Fc/Fc^+ (Table 3, entries 1–7). Reversible anthracene reduction ($E_p \sim -2.0$ V *vs.* SCE) has been reported in both acetonitrile and dimethylformamide;[30] under our conditions, anthracene is reduced at −2.46 V *vs.* Fc/Fc^+.

BN anthracenes **1a–g** are irreversibly oxidized at room temperature in dimethylformamide ($E_{p,a} \sim 0.8$ V *vs.* Fc/Fc^+) and anthracene undergoes rapid oxidative decomposition at even cryogenic temperatures.[31] The short-lived radical cation

Table 2 Onset of absorbance and tabulated optical band gap for compounds in this study[a]

Entry	Compound	Substituent	λ_{onset} [b] (nm)	E_g [c] (eV)
1	**1a**	4-MeO	401	3.09
2	**1b**	4-Me	400	3.10
3	**1c**	4-H	400	3.10
4	**1d**	4-F	399	3.10
5	**1e**	4-Cl	400	3.10
6	**1f**	4-CF_3	401	3.09
7	**1g**	4-CN	396	3.13
8	**1i**	Mes	393	3.15
9	BN anthracene	n/a	392	3.17
10	**8a**	4-H	398	3.12
11	**8b**	4-Me	399	3.11
12	**8c**	4-F	398	3.12
13	Anthracene	n/a	383	3.24

[a] Spectra recorded in tetrahydrofuran at room temperature. [b] λ_{onset} = wavelength of light corresponding to the onset of absorbance. [c] E_g = optical band gap.

 This journal is © The Royal Society of Chemistry 2016

Published on 23 February 2016. Downloaded by Johns Hopkins University on 03/03/2016 18:08:06.

Table 3 Electrochemical data for compounds in this study[a]

Entry	Compound	Substituent	$E_{p,a}$ [b] (V)	$E_{p,c}$ [b] (V)
1	**1a**	4-MeO	0.82	−2.54
2	**1b**	4-Me	0.79	−2.54
3	**1c**	4-H	0.81	−2.52
4	**1d**	4-F	0.91	−2.53
5	**1e**	4-Cl	0.74	−2.48
6	**1f**	4-CF_3	0.85	−2.41
7	**1g**	4-CN	0.88	−2.33
8	**1i**	Mes	0.93	−2.59
9	BN anthracene	n/a	0.77	−2.53
10	**8a**	4-H	0.82	−2.37
11	**8b**	4-Me	0.80	−2.39
12	**8c**	4-F	0.81	−2.37
13	Anthracene	n/a	0.86	−2.46

[a] Data recorded as 3.5 mM solutions in anaerobic, anhydrous dimethylformamide at room temperature with tetrabutylammonium hexafluorophosphate ([Bu_4NPF_6] = 0.1 M) supporting electrolyte under argon. Working electrode = platinum button; counter electrode = platinum wire; reference electrode = $Ag/Ag^+NO_3^-$ in acetonitrile; scan rate = 0.1 V s^{-1}. [b] Relative to Fc/Fc^+ internal standard. Fc = ferrocene; $E_{p,a}$ = peak anodic potential; $E_{p,c}$ = peak cathodic potential.

intermediates are thought to react with solvent, as stable electrochemically generated anthracene cations are observed only at very low temperatures and in very nonnucleophilic solvents.[32] Indeed, we observe additional electrochemically active species in the voltammagram on repeated scans of **1a–g**. As the nitro group is itself redox active, the cyclic voltammagram of compound **1h** is complex (see ESI†).

While the optical spectroscopy of BN anthracenes shows the same onset of absorbance regardless of electron-donating or electron-withdrawing substituents (Fig. 7), and therefore the same HOMO–LUMO gap, electrochemistry can separately probe the HOMO and LUMO energies. We find that the reduction potential becomes less negative with increasing electron-withdrawing character in the series **1a–g**, reflecting a lower lying LUMO level in BN anthracenes with electron-withdrawing substituents. A least-squares fit of the $E_{p,c}$ to the Hammett parameter σ_p is linear (R^2 = 0.89, ρ = −0.22, Fig. 8). The small rho value suggests a modest overall influence of the substituent on the LUMO energy.

The influence of the exocyclic substituent on the peak oxidation potential is less clear-cut. A Hammett analysis shows considerable scatter and a least-squares fit of the $E_{p,a}$ to the Hammett parameter σ_p is not linear (Fig. 8).

Given that these materials have the same optical band gap, but a tunable reduction potential, we predicted that the exocyclic substituent should have an equal effect on the frontier orbitals, lowering the HOMO by an amount equal to the amount by which it lowers the LUMO. Similar results have been observed in triazaborine heterocycles.[33] That we don't observe a linear free energy relationship between substituent and the peak oxidation potential may reflect the rapid decomposition of the BN anthracene radical cation, which results in a broad and unstable peak oxidation potential and contributing to the scatter in the Hammett analysis.

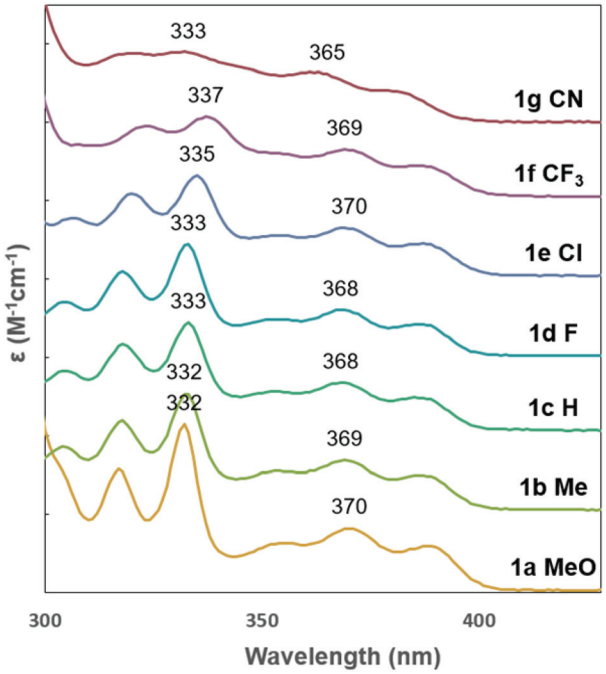

Fig. 7 Absorbance spectroscopy in THF. The extinction coefficient ε in M^{-1} cm^{-1} is plotted *versus* wavelength in nanometers. Spectra are offset for clarity and hash marks represent 10 000 M^{-1} cm^{-1}.

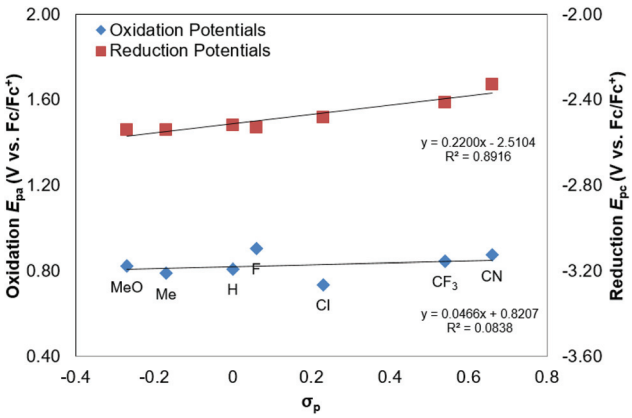

Fig. 8 Potential dependence on BN anthracene electronic properties. Plot of experimentally determined peak reduction potential (red squares) and peak oxidation potential (blue diamonds) *versus* σ_p for BN anthracenes **1a–g**. The black lines represent least squares fits to $f(x) = a + \rho x$.

Electronic structure calculations

To further explore substituent effects absent any decomposition, we turned to DFT calculations. As described earlier, ground state geometry optimization of **1a–g** (CAM B3LYP/6-311G(d,p)) converges on structures in which the exocyclic ring is not coplanar with the anthracene core. This level of theory was selected to allow for direct comparison to Liu's calculations on BN anthracene.[21]

Published on 23 February 2016. Downloaded by Johns Hopkins University on 03/03/2016 18:08:06.

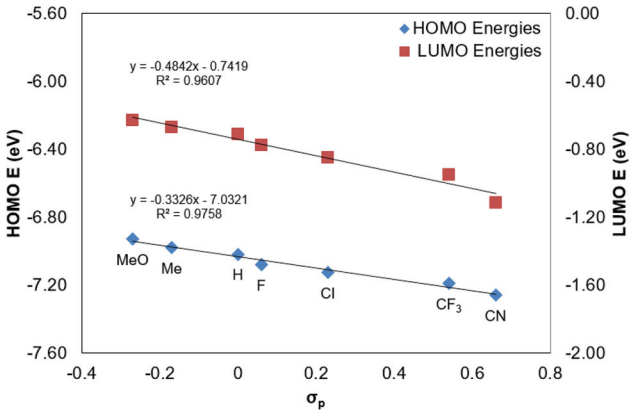

Fig. 9 Frontier molecular orbital energy dependence on BN anthracene electronic properties. Plot of calculated (CAM B3LYP/6-311G(d,p)) LUMO (red squares) and HOMO (blue diamonds) energies *versus* σ_p for BN anthracenes **1a–g**. The black lines represent least squares fits to $f(x) = a + \rho x$.

Comparison of the calculated HOMO and LUMO energies of **1c** and the orbital densities in the optimized geometry (∠ = 25°) and using the crystallographic coordinates (∠ = 7.52°) shows that electronic structure is not strongly conformation dependent (Table S-6†). Since we are not able to isolate diffraction quality crystals for **1a** and **1e**, we carried out the remaining electronic structure calculations using the calculated geometries.

We find a linear free energy relationship between both the calculated HOMO and LUMO energies and the Hammett parameter σ_p (Fig. 9). The slope ρ of the two lines are similar (HOMO: −0.33; LUMO: −0.48) consistent with an equal magnitude substituent effect. The calculated band gaps across the series are also constant (Table S-6†), in agreement with the absorbance spectroscopy.

Conclusions

Our results show that the properties of BN anthracenes closely parallel anthracene and its derivatives. Substituents at the equivalent of the 2-position of anthracene have a small but measurable influence on electronic properties, without perturbing bulk structure. These conclusions enable predictions about structure–function relationships in azaborine derivatives. For example, given that in anthracene peripheral functionalization at the 9,10 positions is of particular interest for materials applications, our results highlight the desirability of more synthetic methods increasing the chemical and structural diversity of extended BN materials.

Experimental

General experimental procedures

All reactions were conducted under a positive pressure of inert atmosphere (nitrogen or argon), unless stated otherwise. Standard Schlenk techniques were used in all syntheses conducted under inert atmosphere and all glassware was oven-dried overnight in a 175 °C oven. ^{1}H NMR, ^{11}B NMR, ^{13}C {^{1}H} NMR, and ^{19}F {^{1}H} NMR spectra were recorded on a Bruker Avance III 400 MHz Spectrometer and chemical shifts are reported in parts per million (ppm). Spectra were recorded in chloroform-*d*, dichloromethane-d_2, or DMSO-d_6, with the residual solvent peak as the internal standard (^{1}H NMR: $CHCl_3$, δ = 7.26 ppm; CH_2Cl_2, δ = 5.32 ppm. ^{13}C NMR: $CHCl_3$, δ = 77.16 ppm; CH_2Cl_2, δ = 53.84 ppm; DMSO, δ = 39.52 ppm). ^{11}B NMR spectra are externally referenced to boron trifluoride diethyl etherate ($BF_3{\cdot}Et_2O$, δ = 0 ppm). ^{19}F {^{1}H} NMR spectra are reported as collected. Carbons bound to boron are not observed due to the quadrupolar relaxation of boron. Low-resolution Mass Spectrometry and High Resolution Mass Spectrometry were performed in the Department of Chemistry at Johns Hopkins University using a VG Instruments VG70S/E magnetic sector mass spectrometer with EI (70 eV).

Synthesis of BN anthracenes 1a–h.[6] An oven dried 15 mL heavy walled cylindrical pressure vessel equipped with a stir bar was charged with **4** (1 equiv., 1.8 mmol, 304 mg) and the appropriate potassium aryltrifluoroborate (0.8 equiv., 1.5 mmol). The vessel and contents were brought into a nitrogen atmosphere glove box. Toluene (6 mL), cyclopentyl methyl ether (CPME) (6 mL), triethylamine (1.5 equiv., 2.3 mmol, 0.32 mL), and silicon tetrachloride (1 equiv., 1.5 mmol, 175 μL) were added to the reaction vessel. The vessel was sealed with a PTFE screw cap, brought out of the glove box and heated to 100 °C for 18 hours with stirring. The reaction mixture was cooled to room temperature, added to a separatory funnel, and diluted with an aqueous hydrochloric acid solution (1 M, 30 mL) and ethyl acetate (25 mL). The organic layer was collected and the aqueous layer was washed with ethyl acetate (3 × 25 mL). The combined organic layers were washed with a saturated aqueous sodium bicarbonate solution (1 × 50 mL) then a saturated aqueous sodium chloride solution (1 × 50 mL), dried over anhydrous sodium sulfate, and concentrated by rotary evaporation under reduced pressure. The products were recrystallized from hot chlorobenzene. (In exception to this procedure was the work-up of **1h**, as detailed in the ESI.†)

2-(4-Methoxyphenyl)-1,2-dihydronaphtho[2,3-*e*][1,2]-azaborinine (1a). 0.11 g, 25% yield. ^{1}H NMR (400 MHz, $CDCl_3$): δ 8.24 (1 H, d, *J* 11.7), 8.17 (1 H, s), 8.05 (1 H, s), 7.99–7.92 (3 H, m), 7.88 (1 H, d, *J* 8.4), 7.73 (1 H, s), 7.50 (1 H, ddd, *J* 8.3, 6.7, 1.3), 7.41 (1 H, ddd, *J* 8.0, 6.7, 1.2), 7.10–7.04 (2 H, m), 3.92 (3 H, s). ^{13}C NMR (101 MHz, DMSO-d_6): δ 160.99, 144.90, 139.20, 135.33, 132.98, 127.99, 127.97, 126.50, 126.27, 126.13, 123.45, 113.59, 113.25, 54.97. ^{11}B NMR (128 MHz, $CDCl_3$) δ 34.10. HRMS (EI) *m*/*z*: $[M]^+$ Calcd for $C_{19}H_{16}BNO$ 285.1325; Found 285.13217.

2-(*p*-Tolyl)-1,2-dihydronaphtho[2,3-*e*][1,2]azaborinine (1b). 0.077 g, 19% yield. ^{1}H NMR (400 MHz, $CDCl_3$): δ 8.23 (1 H, d, *J* 11.6), 8.16 (1 H, s), 8.09 (1 H, s), 7.94 (1 H, d, *J* 8.2), 7.88 (2 H, d, *J* 7.9), 7.89–7.82 (1 H, m), 7.72 (1 H, s), 7.48 (1 H, ddd, *J* 8.2, 6.7, 1.3), 7.39 (1 H, ddd, *J* 8.1, 6.7, 1.2), 7.35–7.27

 This journal is © The Royal Society of Chemistry 2016

Published on 23 February 2016. Downloaded by Johns Hopkins University on 03/03/2016 18:08:06.

(3 H, m), 2.43 (3 H, s). ^{13}C NMR (101 MHz, DMSO-d_6): δ 145.14, 139.45, 139.10, 133.69, 132.97, 128.68, 128.05, 128.03, 128.02, 126.56, 126.31, 126.19, 123.54, 113.45, 21.22. ^{11}B NMR (128 MHz, $CDCl_3$): δ 34.84. HRMS (EI) *m*/*z*: $[M]^+$ Calcd for $C_{19}H_{16}BN$ 269.1376; Found 269.13806.

2-Phenyl-1,2-dihydronaphtho[2,3-*e*][1,2]azaborinine (1c). 0.17 g, 44% yield. ^{1}H NMR (400 MHz, $CDCl_3$): δ 8.26 (1 H, d, *J* 11.6), 8.18 (1 H, s), 8.13 (1 H, s), 8.01–7.84 (4 H, m), 7.74 (1 H, s), 7.55–7.46 (4 H, m), 7.40 (1 H, ddd, *J* 8.1, 6.7, 1.2), 7.29 (1 H, dd, *J* 11.7, 1.9). ^{13}C NMR (101 MHz, DMSO-d_6): δ 145.34, 139.02, 133.59, 133.59, 130.28, 129.89, 128.11, 128.09, 128.03, 127.96, 126.591, 126.35, 126.19, 123.60, 113.60. ^{11}B NMR (128 MHz, $CDCl_3$): δ 34.62. HRMS (EI) *m*/*z*: $[M]^+$ Calcd for $C_{18}H_{14}BN$ 255.1219; Found 255.12272.

2-(4-Fluorophenyl)-1,2-dihydronaphtho[2,3-*e*][1,2]-azaborinine (1d). 0.22 g, 54% yield. ^{1}H NMR (400 MHz, $CDCl_3$): δ 8.25 (1 H, d, *J* 11.6), 8.17 (1 H, s), 8.06 (1 H, s), 7.98–7.91 (3 H, m), 7.89–7.84 (1 H, m), 7.73 (1 H, s), 7.50 (1 H, ddd, *J* 8.2, 6.7, 1.3), 7.40 (1 H, ddd, *J* 8.1, 6.7, 1.2), 7.26–7.16 (3 H, m). ^{13}C NMR (101 MHz, DMSO-d_6) δ 164.20 (d, *J* 246.9), 145.88, 139.42, 136.50, 136.42, 133.46, 128.62, 128.57, 128.50, 127.07, 126.85, 126.57, 124.11, 115.49, 115.29, 114.02. ^{11}B NMR (128 MHz, $CDCl_3$) δ 34.42. ^{19}F NMR (376 MHz, $CDCl_3$): δ −110.75. HRMS (EI) *m*/*z*: $[M]^+$ Calcd for $C_{18}H_{13}BFN$ 273.1125; Found 273.11224.

2-(4-Chlorophenyl)-1,2-dihydronaphtho[2,3-*e*][1,2]azaborinine (1e). 0.30 g, 70% yield. ^{1}H NMR (400 MHz, $CDCl_3$): δ 8.26 (1 H, d, *J* 11.7), 8.18 (1 H, s), 8.09 (1 H, s), 7.95 (1 H, ddd, *J* 8.3, 1.4, 0.7), 7.91–7.84 (3 H, m), 7.74 (1 H, s), 7.54–7.45 (3 H, m), 7.41 (1 H, ddd, *J* 8.1, 6.7, 1.2), 7.23 (1 H, dd, *J* 11.6, 2.0). ^{13}C NMR (101 MHz, DMSO-d_6): δ 145.59, 138.85, 135.46, 134.98, 132.99, 128.25, 128.15, 128.05, 128.02, 126.64, 126.42, 126.14, 123.71, 113.68, 113.64. ^{11}B NMR (128 MHz, $CDCl_3$): δ 34.31. HRMS (EI) *m*/*z*: $[M]^+$ Calcd for $C_{18}H_{13}BClN$ 289.083; Found 289.08337.

2-(4-(Trifluoromethyl)phenyl)-1,2-dihydronaphtho[2,3-*e*][1,2]-azaborinine (1f). 0.22 g, 46% yield. ^{1}H NMR (400 MHz, $CDCl_3$): δ 8.31 (1 H, d, *J* 11.6), 8.21 (1 H, d, *J* 1.0), 8.17 (1 H, s), 8.08–8.02 (2 H, m), 7.99–7.94 (1 H, m), 7.92–7.86 (1 H, m), 7.78 (1 H, s), 7.77–7.71 (2 H, m), 7.54–7.48 (1 H, m), 7.42 (1 H, ddd, *J* 8.1, 6.7, 1.2), 7.26 (1 H, dd, *J* 11.6, 2.0). ^{13}C NMR (101 MHz, DMSO-d_6): δ 146.39, 139.17, 134.67, 133.47, 130.48, 130.16, 128.77, 128.72, 128.54, 127.16, 126.95, 126.65, 126.28, 124.92, 124.88, 124.30, 123.57, 114.37. ^{11}B NMR (128 MHz, $CDCl_3$): δ 34.53. ^{19}F NMR (376 MHz, $CDCl_3$): δ −62.76. HRMS (EI) *m*/*z*: $[M]^+$ Calcd for $C_{19}H_{13}BF_3N$ 323.1093; Found 323.10941.

4-(Naphtho[2,3-*e*][1,2]azaborinin-2(1*H*)-yl)benzonitrile (1g). 0.062 g, 15% yield. ^{1}H NMR (400 MHz, $CDCl_3$): δ 8.36–8.28 (1 H, m), 8.21 (1 H, s), 8.16 (1 H, s), 8.04–7.99 (2 H, m), 7.92 (2 H, dddtd, *J* 32.0, 8.4, 1.3, 0.8), 7.80–7.73 (3 H, m), 7.48 (2 H, dddd, *J* 34.5, 8.1, 6.7, 1.2), 7.22 (1 H, dd, *J* 11.6, 2.0). ^{13}C (101 MHz, DMSO): δ 146.01, 138.61, 134.18, 132.99, 131.44, 128.32, 128.28, 128.06, 126.70, 126.50, 126.17, 123.88, 119.09, 113.95, 112.05. ^{11}B (128 MHz, $CDCl_3$): δ 34.06. HRMS (EI) *m*/*z*: $[M]^+$ Calcd for $C_{19}H_{13}BN_2$ 280.1172; Found 280.11689.

2-(4-Nitrophenyl)-1,2-dihydronaphtho[2,3-*e*][1,2]azaborinine (1h). 0.27 g, 59% yield. ^{1}H NMR (400 MHz, $CDCl_3$): δ 8.37–8.30 (3 H, m), 8.23 (1 H, s), 8.21 (1 H, s), 8.12–8.07 (2 H, m), 8.00–7.86 (2 H, m), 7.80 (1 H, s), 7.48 (2 H, dddd, *J* 34.4, 8.1, 6.7, 1.2), 7.25 (1 H, dd, *J* 11.8, 1.8). ^{13}C NMR (101 MHz, DMSO): δ 148.38, 146.07, 138.58, 134.70, 133.00, 130.25, 128.36, 128.34, 128.31, 128.06, 126.98, 126.71, 126.51, 126.16, 123.90, 122.50, 122.48, 114.05. ^{11}B NMR (128 MHz, $CDCl_3$): δ 34.26. HRMS (EI) *m*/*z*: $[M]^+$ Calcd for $C_{18}H_{13}BN_2O_2$ 300.107; Found 300.10714.

Acknowledgements

We thank Johns Hopkins University for start-up funds. We thank Prof. J. D. Tovar and research group for the use of their spectrometer and Prof. Sara Thoi for helpful discussion of electrochemical techniques.

Notes and references

1 P. v. R. Schleyer, *Chem. Rev.*, 2001, **101**, 1115.
2 M. J. S. Dewar, V. P. Kubba and R. Pettit, *J. Chem. Soc.*, 1958, 3073.
3 P. G. Campbell, S.-Y. Liu and A. J. V. Marwitz, *Angew. Chem., Int. Ed.*, 2012, **51**, 6074.
4 A. J. V. Marwitz, M. H. Matus, L. N. Zakharov, D. A. Dixon and S.-Y. Liu, *Angew. Chem., Int. Ed.*, 2009, **48**, 973.
5 A. J. Ashe and X. Fang, *Org. Lett.*, 2000, **2**, 2089.
6 S. R. Wisniewski, C. L. Guenther, O. A. Argintaru and G. A. Molander, *J. Org. Chem.*, 2014, **79**, 365.
7 G. A. Molander and S. R. Wisniewski, *J. Org. Chem.*, 2014, **79**, 6663.
8 A. Chrostowska, S. Xu, A. N. Lamm, A. Maziere, C. D. Weber, A. Dargelos, P. Baylere, A. Graciaa and S.-Y. Liu, *J. Am. Chem. Soc.*, 2012, **134**, 10279.
9 A. Chrostowska, S. Xu, A. Maziere, K. Boknevitz, E. R. Abbey, A. Dargelos, A. Graciaa and S. Y. Liu, *J. Am. Chem. Soc.*, 2014, **136**, 11813.
10 P. G. Campbell, L. N. Zakharov, D. J. Grant, D. A. Dixon and S.-Y. Liu, *J. Am. Chem. Soc.*, 2010, **132**, 3289.
11 T. Agou, J. Kobayashi and T. Kawashima, *Org. Lett.*, 2006, **8**, 2241.
12 X.-Y. Wang, H.-R. Lin, T. Lei, D.-C. Yang, F.-D. Zhuang, J.-Y. Wang, S.-C. Yuan and J. Pei, *Angew. Chem., Int. Ed.*, 2013, **52**, 3117.
13 E. R. Abbey and S.-Y. Liu, *Org. Biomol. Chem.*, 2013, **11**, 2060.
14 D. H. Knack, J. L. Marshall, G. P. Harlow, A. Dudzik, M. Szaleniec, S.-Y. Liu and J. Heider, *Angew. Chem., Int. Ed.*, 2013, **52**, 2599.
15 D. Bonifazi, F. Fasano, M. M. Lorenzo-Garcia, D. Marinelli, H. Oubaha and J. Tasseroul, *Chem. Commun.*, 2015, **51**, 15222.

Published on 23 February 2016. Downloaded by Johns Hopkins University on 03/03/2016 18:08:06.

16 X.-Y. Wang, J.-Y. Wang and J. Pei, *Chem. – Eur. J.*, 2015, **21**, 3528.
17 A. Narita, X.-Y. Wang, X. Feng and K. Mullen, *Chem. Soc. Rev.*, 2015, **44**, 6616.
18 L. Zhiqiang and T. B. Marder, *Angew. Chem., Int. Ed.*, 2008, **47**, 242.
19 S. Sanyal, A. K. Manna and S. K. Pati, *J. Mater. Chem. C*, 2014, **2**, 2918.
20 M. J. S. Dewar and R. Dietz, *J. Chem. Soc.*, 1959, 2728.
21 J. S. A. Ishibashi, J. L. Marshall, A. Mazière, G. J. Lovinger, B. Li, L. N. Zakharov, A. Dargelos, A. Graciaa, A. Chrostowska and S.-Y. Liu, *J. Am. Chem. Soc.*, 2014, **136**, 15414.
22 D. M. Knapp, E. P. Gillis and M. D. Burke, *J. Am. Chem. Soc.*, 2009, **131**, 6961.
23 J.-M. Valk, R. van Belzen, J. Boersma, A. L. Spek and G. van Koten, *J. Chem. Soc., Dalton Trans*, 1994, 2293.
24 R. Islas, E. Chamorro, J. Robles, T. Heine, J. C. Santos and G. Merino, *Struct. Chem.*, 2007, **18**, 833.
25 *CRC Handbook of Chemistry and Physics*, 96th edn, 2015, p. 9-1.
26 A. M. Mathieson, J. M. Robertson and V. C. Sinclair, *Acta Cryst.*, 1950, **3**, 245.
27 J. E. Anthony, *Angew. Chem., Int. Ed.*, 2008, **47**, 452.
28 H. Chiba, J. Nishida and Y. Yamashita, *Chem. Lett.*, 2012, **41**, 482.
29 F. Valiyev, W.-S. Hu, H.-Y. Chen, M.-Y. Kuo, I. Chao and Y.-T. Tao, *Chem. Mater.*, 2007, **19**, 3018–3026.
30 *CRC Handbook of Chemistry and Physics*, 96th edn, 2015, pp. 5–90.
31 L. Byrd, L. L. Miller and D. Pletcher, *Tetrahedron Lett.*, 1972, **13**, 2419.
32 M. Dietrich, J. Mortensen and J. Heinze, *Angew. Chem., Int. Ed.*, 1985, **24**, 508.
33 F. Josefík, T. Mikysek, M. Svobodová, P. Šimůnek, H. Kvapilová and J. Ludvík, *Organometallics*, 2014, **33**, 4931.

 This journal is © The Royal Society of Chemistry 2016